

Total Anuria in an Infant with Rotavirus Gastroenteritis: Differential Diagnosis Between Bilaterally Obstructing Ammonium Acid Urate (AAU) Stones and Bilateral Papillary Necrosis

Amos Neheman MD¹, Ze'ev Korzets MBBS^{2,5}, Rodica Stackievicz MD³, Tomer Itzhaki MD², Giulia Pula MD¹, Galit Pomeranz MD¹, Meidad Greenberg MD¹, Dganit Adam MD⁴ and Avishalom Pomeranz MD^{1,5}

¹Unit of Pediatric Urology, ²Unit of Pediatric Nephrology, ³Department of Radiology and ⁴Unit of Pediatric Intensive Care, Meir Medical Center, Kfar Saba, Israel

⁵Sackler Faculty of Medicine, Tel Aviv University, Tel Aviv, Israel

KEY WORDS: anuria, rotavirus gastroenteritis, ammonium acid urate stones (AAU), papillary necrosis

IMAJ 2017; 19: 654–656

Total anuria due to obstructive uropathy is rarely seen in the pediatric population. Rotavirus is among the most common pathogens causing acute gastroenteritis in childhood, primarily in children younger than 5 years of age. Of late, rotavirus gastroenteritis has been reported to be associated with acute post-renal failure due to bilateral ureteric obstruction by renal calculi. Specifically, the stones formed in this setting consist of ammonium acid urate (AAU), an extremely rare component of all urolithiasis patients. The diagnosis of AAU stones may, however, be difficult to definitively establish as other causes of ureteric obstruction must be excluded. In particular, bilateral papillary necrosis can present in an identical manner.

We report on an infant who developed total anuria due to bilateral ureteric obstruction during the course of rotavirus gastroenteritis. The differential diagnosis between AAU calculi and bilateral papillary necrosis is discussed. Following the insertion of bilateral ureteric double J stents, renal function was fully recovered.

PATIENT DESCRIPTION

An 18 month old male infant was admitted after a 6 day history of vomiting and diarrhea. On examination, he showed signs of severe dehydration. Laboratory data revealed a serum creatinine level of 0.9 mg/dl, urea 39 mg/dl, and uric acid 11.2 mg/dl. Urinalysis was positive for blood (red blood cells 200/ μ l), protein 100 mg/dl, and trace ketones. Urine pH was 5.5 and urine specific gravity 1.025. Blood gas analysis showed a pH of 7.33 with a HCO₃ of 15 mmol/L and a pCO₂ of 28.7 mmHg. The child was aggressively rehydrated. Despite volume resuscitation, over the next 24 hours, he became totally anuric with serum creatinine peaking at 2.2 mg/dl. Renal ultrasonography displayed mildly enlarged kidneys with moderate bilateral calyceal and pelvic dilatation. Hyperechogenic debris of an undefined nature was seen in the calyces of the right kidney [Figure 1A, Figure 1B] and in the left collecting system.

This same hyperechogenic, "soft tissue-like" material was also detected in the urinary bladder [Figure 1C]. A non-contrast computed tomography (NCCT) confirmed the presence of bilateral hydronephrosis but failed to depict stones in the calyces of the right kidney. Soft-tissue attenuation (15–30 HU) material was seen in the right renal calyces and proximal ureter. A small amount of high attenuation matter was present at the left ureterovesical junction [Figure 1D, Figure 1E].

Cystoscopy and retrograde contrast imaging confirmed bilateral ureteric obstruction. At endoscopy, there was a "snow-storm" appearance in the bladder with caseous debris emerging from both ureteric orifices. The debris was partially disintegrated and dislodged by the introduction of the retrograde catheters.

Continued postoperative ureteric drainage was ensured by the insertion of double J stents with a resulting prompt diuresis and a rapid (within 48 hours) normalization of serum creatinine to 0.4 mg/dl.

Histological examination of the "cola-colored" urine drained during stent insertion was non-specific, showing only reactive and atypical epithelial cells.

Unfortunately, the expelled debris was not submitted to a biochemical analysis.

The upper tract dilatation improved progressively and the ureteric stents were removed after 4 weeks. A repeat ultrasound of the kidneys following stent removal showed complete disappearance of the hyperechogenic material but persistent calyceal dilatation more evident in the upper pole of the right kidney [Figure 1F].

Notably, rotavirus antigen in the stool returned positive.

COMMENT

Our reported infant contracted rotavirus gastroenteritis leading to a prolonged period of vomiting and diarrhea with resul-

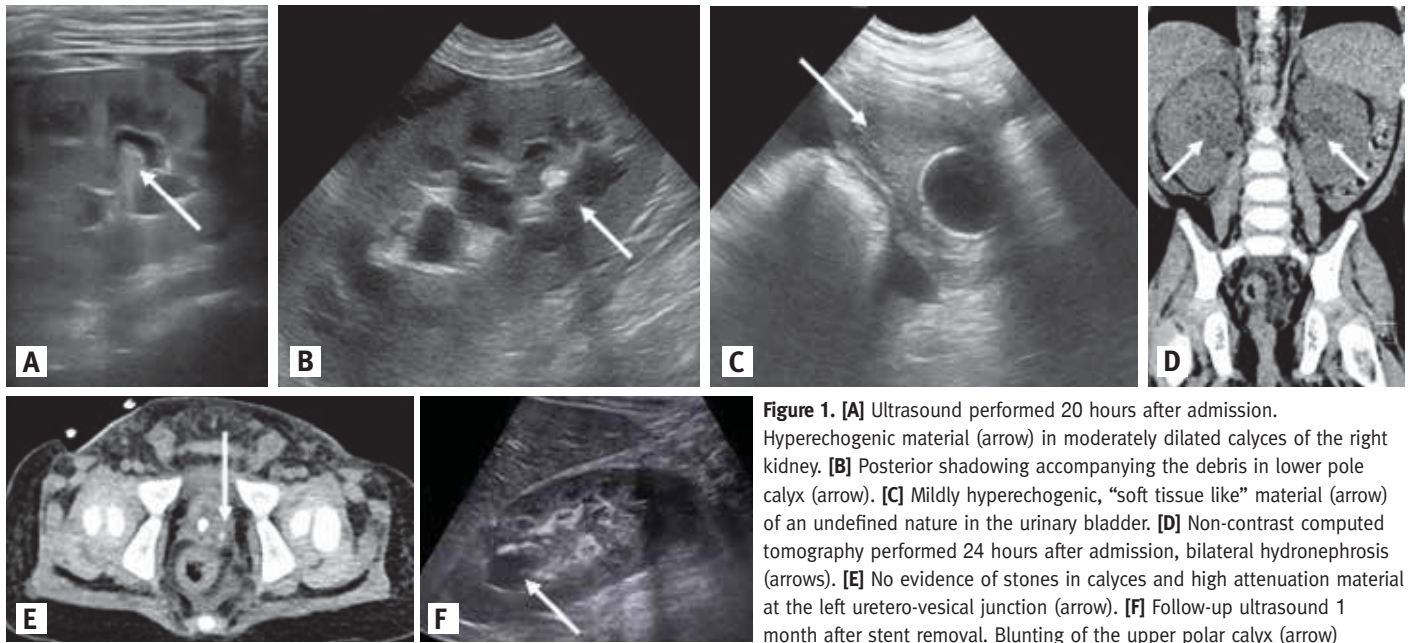


Figure 1. [A] Ultrasound performed 20 hours after admission. Hyperechogenic material (arrow) in moderately dilated calyces of the right kidney. [B] Posterior shadowing accompanying the debris in lower pole calyx (arrow). [C] Mildly hyperechogenic, “soft tissue like” material (arrow) of an undefined nature in the urinary bladder. [D] Non-contrast computed tomography performed 24 hours after admission, bilateral hydronephrosis (arrows). [E] No evidence of stones in calyces and high attenuation material at the left uretero-vesical junction (arrow). [F] Follow-up ultrasound 1 month after stent removal. Blunting of the upper polar calyx (arrow)

tant severe dehydration. Acute pre-renal failure would be the obvious diagnostic choice as a cause of his impaired renal function. However, he went on to develop total anuric renal failure due to bilateral ureteric obstruction. Such rotavirus gastroenteritis-induced post-renal failure has recently been reported and appears to be especially prevalent in Japan [1,2]. The obstruction is caused by the formation of AAU renal calculi. AAU are extremely rare kidney stone components accounting for only 0.38% of all urolithiasis cases in Japan [2]. The pathophysiology of AAU stone formation remains to be elucidated. Hyperuricemia, hyperuricosuria, and metabolic acidosis, which is secondary to dehydration, have been speculated to play a role. Thus, severe volume depletion and electrolyte loss lead to intracellular acidosis and increased excretion of urinary ammonium. The low urinary sodium allows for the coupling of urate with the abundant ammonium ion promoting the formation of AAU stones. Kamei et al. [3] described a 7 month old boy with hereditary hypouricemia due to a homozygous nonsense mutation of the urate transporter 1 gene who developed acute kidney injury during the course of rotavirus gastroenteritis. This patient,

although exhibiting an increased uric acid excretion, did not show evidence of either hydronephrosis or stones. In other reports of AAU stone formation, hyperuricosuria has not been documented [2]. Although AAU stones have almost exclusively been associated with rotavirus gastroenteritis, a similar scenario has been described with norovirus gastroenteritis [4].

Our patient’s clinical course was similar to the cases presented in these mentioned reports. However, our imaging findings differed. Whereas in those cases, NCCT demonstrated findings characteristic of renal stones (hyperdense foci along the collecting system), in our patient computed tomography (CT) detected soft tissue attenuation material located at the site of presumed stones as visualized by ultrasound. The only known soft-tissue attenuation stones found on CT scans are indinavir and pure matrix stones.

The disappearance of debris seen on ultrasound and NCCT and the rapid recovery of renal function following double J stenting are akin to any acute obstructive uropathy once the obstructing element is either removed or bypassed. Unfortunately, in our case the expelled ureteric debris was not subjected to chemical analysis. The

cola-colored urinary sediment contained only atypical epithelial cells. No “haw-like” (i.e., AAU) crystals were identified. Typically, AAU stones are described as brown sandy stones. Despite the lack of a definitive chemical analysis and the non-specific urinary sediment, the macroscopic appearance of the expelled debris and sediment is in keeping with that of AAU stones.

As expected, hydronephrosis regressed. However, contrary to expectations, calyceal dilatation with a clubbing appearance of some calyces persisted. This condition led us to consider the other possible diagnoses in our patient, namely, bilateral papillary necrosis. The basic underlying pathophysiology of papillary necrosis is ischemia of the papillae. The most common causes are analgesic abuse (inclusive of non-steroidal anti-inflammatory drugs), sickle cell disease, diabetes mellitus, and infection (pyelonephritis, tuberculosis). None of these pertained to our patient. In the pediatric literature, anecdotal cases of papillary necrosis have been reported in association with dehydration, septicemia, and asphyxia. They most commonly occur in infants and small children.

Gordon and colleagues [5] described a 9 year old girl with meningococcal septic-

mia who developed complete bilateral ureteral obstruction due to sloughed necrotic papillae. Their report is remarkably similar to our case, apart from the offending infectious pathogen.

Differentiating between the two diagnoses we have raised is virtually impossible without the performance of either an intravenous pyelography or contrast enhanced CT. As the child is fully recovered now, we feel that carrying out either of these imaging studies would be unethical.

CONCLUSION

In conclusion, total anuria due to bilateral ureteric obstruction is a rare event in children. In the setting of rotavirus gastroenteritis, formation of AAU renal stones should be considered. The other differential diagnosis to be considered is bilateral papillary necrosis.

Correspondence

Dr. A. Pomeranz

Dept. of Pediatric Nephrology, Meir Medical Center, Kfar Saba 44281, Israel

Phone: (972-9) 747-2416, **Fax:** (972-9) 742-5967

email: apclinic@zahav.net.il

References

1. Kira S, Mitsui T, Zakoji H, et al. Postrenal failure due to urinary stones associated with acute viral gastroenteritis: Three case reports. *Case Rep Urol* 2016; 2016: 1375923. Published online 26 Oct 2016.
2. Yokoyama T, Sugimoto N, Kato E, et al. Rotavirus gastroenteritis-associated urinary ammonium acid urate crystals. *Pediatr Int* 2015; 57: 158-60.
3. Kamei K, Ogura M, Ishimori S, et al. Acute kidney injury after acute gastroenteritis in an infant with hereditary hypouricemia. *Eur J Pediatr* 2014; 173: 247-9.
4. Ashida A, Shirasu A, Nkakura H, Tamai H. Acute renal failure due to obstructive urate stones associated with norovirus gastroenteritis. *Pediatr Nephrol* 2010; 25: 2377-78.
5. Gordon M, Raimondo MC, Postlethwaite R, et al. Acute renal papillary necrosis with complete bilateral ureteral obstruction in a child. *Urology* 2007; 69: 575e11-2.

Capsule

Plasmodium leftovers cause bone loss

Malaria patients sometimes develop long-term consequences of infection, such as bone loss and growth retardation. Lee and colleagues found that the *Plasmodium* by-product hemozoin can remain in the bone marrow and cause bone loss. Mice infected with a mutant *Plasmodium* that did not produce hemozoin did not undergo bone loss. Hemozoin-

induced inflammatory responses in osteoclast and osteoblast precursors, resulting in bone resorption. Treating infected animals with alfacalcidol, a vitamin D3 analog, prevented this bone loss.

Sci Immunol 2017; 2: eaam8093

Eitan Israeli

Capsule

Habitual coffee consumption and genetic predisposition to obesity: gene–diet interaction analyses in three U.S. prospective studies

Whether habitual coffee consumption interacts with the genetic predisposition to obesity in relation to body mass index (BMI) and obesity is unknown. Wang and colleagues analyzed the interactions between genetic predisposition and habitual coffee consumption in relation to BMI and obesity risk in 5116 men from the Health Professionals Follow-up Study (HPFS), in 9841 women from the Nurses' Health Study (NHS), and in 5648 women from the Women's Health Initiative (WHI). The genetic risk score was calculated based on 77 BMI-associated loci. Coffee consumption was examined prospectively in relation to BMI. The genetic association with BMI was attenuated among participants with higher consumption of coffee than among those with lower consumption in the HPFS ($P_{interaction} = 0.023$) and NHS ($P_{interaction} = 0.039$); similar results were replicated in the WHI ($P_{interaction} = 0.044$). In the combined data of all cohorts, differences in BMI per increment of 10-risk allele were 1.38 (standard error [SE], 0.28), 1.02 (SE, 0.10), and 0.95 (SE, 0.12) kg/m² for coffee consumption of <1, 1–3 and >3 cup(s)/day,

respectively ($P_{interaction} < 0.001$). Such interaction was partly due to slightly higher BMI with higher coffee consumption among participants at lower genetic risk and slightly lower BMI with higher coffee consumption among those at higher genetic risk. Each increment of 10-risk allele was associated with 78% (95% confidence interval [CI], 59–99%), 48% (95%CI, 36–62%), and 43% (95%CI, 28–59%) increased risk for obesity across these subgroups of coffee consumption ($P_{interaction} = 0.008$). From another perspective, differences in BMI per increment of 1 cup/day coffee consumption were 0.02 (SE, 0.09), -0.02 (SE, 0.04), and -0.14 (SE, 0.04) kg/m² across tertiles of the genetic risk score. The authors concluded that higher coffee consumption might attenuate the genetic associations with BMI and obesity risk, and individuals with greater genetic predisposition to obesity appeared to have lower BMI associated with higher coffee consumption.

BMC Med 2017; 15: 97

Eitan Israeli

“To thrive in life you need three bones. A wishbone. A backbone. And a funny bone”

Reba McEntire, (born 1955), an American singer, songwriter, actress, and record producer